GSA Data Repository 2017260 doi:10.1130/G39296.1

Rapid time scale of Earth's youngest known ultrahigh-pressure metamorphic event, Papua New Guinea

Joel W. DesOrmeau, Stacia M. Gordon, Timothy A. Little, Samuel A. Bowring, and Nilanjan Chatterjee

Tables DR1–DR4

Mailolo Dome Eclogite PNG08-010f

Phengite eclogite (PNG08-010f), collected from the coesite locality on Tumabaguna Island, consists mainly of elongate garnet and omphacite that define a weak foliation. The overall mineral-phase proportions preserved in PNG08-010f are ~47% omphacite, ~34% garnet ~13% quartz, ~3% phengite, ~2% rutile, and <<0.5% amphibole and epidote. Interstitial quartz and minor phengite, with accessory phases apatite, rutile, and zircon, are found as inclusions and in textural equilibrium with garnet and omphacite. Minor symplectite growth of diopsidic clinopyroxene and/or amphibole and albite occurs along rims of garnet, omphacite, and phengite. Rare amphibole, ferro-taramite–taramite, is preserved as inclusions in garnet and locally is associated with breakdown reactions forming muscovite, quartz, plagioclase, and alunite. The well-preserved UHP peak assemblage consists of garnet + omphacite + coesite/quartz + phengite + rutile. Garnet contains inclusions of phengite, rutile, zircon, and rare amphibole. The subhedral to anhedral garnets are typically 0.1–0.5 mm across and exhibit a very limited range of compositions: $Alm_{58–61}Prp_{22–24}Grs_{16–19}Sps_{1}$ (Table DR1). Omphacite is subhedral to anhedral, typically 0.8 mm across, has sodic-rich compositions ($Jd_{63–68}$), and occurs as the main matrix phase. Larger omphacite grains (3.5 mm in length) are also found in the sample and have the same composition. Phengite occurs as tabular grains that are typically 0.7 mm in length and some rims show minor retrogression to fine-grained biotite and plagioclase. The grains are weakly zoned, with a decrease in celadonite component from core to rim. In addition, the phengite show a range in Si from 3.33–3.51 atoms per formuls unit (a/fu), but typical matrix grains have Si = 3.33–3.43 a/fu (Table DR1). Quartz occurs within the matrix and as inclusions within garnet and adjacent omphacite that are associated with distinct radial fractures. Zircons extracted from the fresh matrix of this eclogite contain inclusions of the peak assemblage, including omphacite, garnet, rutile, and rare phengite (FIG. 2A). The ~5–10 μm inclusions of omphacite and garnet have identical compositions to matrix omphacite (Jd_{66}) and garnet ($Alm_{59}Prp_{23}Grs_{18}Sps_{1}$) (Table DR1), indicating zircon growth during peak metamorphic mineral crystallization from ca. 6.0–5.2 Ma.

Electron-microprobe analysis of major phases

Mineral compositions were measured by electron-microprobe analysis with a JEOL JXA-8200 Superprobe at the Massachusetts Institute of Technology using an accelerating voltage of 15 kV and a beam current of 10 nA. Spots for garnet, clinopyroxene (omphacite), and phengite analyses were selected using backscattered electron (BSE) images and EDS compositional maps of relevant textural areas related to fresh and minor retrogressed portions of the thin section; the BSE and EDS maps were collected using a JEOL 7100 field emission scanning electron microscope at the University of Nevada, Reno. Mineral compositional data were recalculated with the program AX (Holland, 2009) to standard numbers of oxygen a/fu for anhydrous minerals (Deer et al., 1992). Phengite and amphibole analyses were calculated to a total of 11 and 23 oxygens pfu, respectively. The Fe^{3+}/Fe^{total} in amphibole analyses were first calculated with an excel spreadsheet to classify amphiboles (Locock, 2014) based on IMA 2012 recommendations that uses a scoring criteria of four cation sum procedures: 1) sum of all cations from Si to K = 16 a/fu; 2) sum of cations from Si to Na = 15 a/fu; 3) sum of cations (includes Li) from Si to Ca = 15 a/fu; and 4) sum of cations (includes Li) from Si to Mg = 13a/fu (Hawthorne et al., 2012) used in the amphibole normalization. The best scores are given to normalization schemes that have the smallest maximum deviations from the formula proportions (Locock, 2014). As a check, recalculated amphibole analyses with the best scoring criteria were confirmed by comparing the compositions to the same analyses recalculated by the Holland and Blundy (1994) procedure implemented in AX (Holland, 2009). This technique assumes all Fe in the 23-oxygen normalization to be ferrous and then determines a Fe^{3+} content that falls in the center of a range that satisfies eight independent crystal-chemical constraints. Garnet and omphacite Fe^{3+}/Fe^{Total} proportions were recalculated in AX based on 8 cations per 12 oxygens and 4 cations per 6 oxygens, respectively. Representative analyses of all garnet, clinopyroxene, phengite, and minor amphibole are given in Table DR1. Mineral chemistry plots of garnet and clinopyroxene are presented in Figure 2A. Mineral abbreviations are after Whitney and Evans (2010).

P–T pseudosection modeling

The effective bulk-rock composition used in this study was determined by combining compositional analyses of homogenous major phases, including estimates of Fe^{3+}/Fe^{Total} for garnet and omphacite, and their volume proportions currently preserved in the rock using the estimates previously described (see Mailolo Dome Eclogite PNG08-010f section above). Volume proportions of major phases were estimated from BSE and EDS area maps of the thin section and from petrography (e.g. Carson et al., 1999; Indares et al., 2008, Palin et al., 2015). Phase-diagram pseudosections were calculated with the software Perple_X (Connolly, 2005; version 6.7.0 Jan. 2015) and the Paralyzer tool (Mark Caddick, VT), using the internally consistent thermodynamic dataset of Holland and Powell (1998, hp02ver.dat). The pseudosections were calculated for the system Na_2O-CaO-FeO-MgO-K_2O-MnO-Al_2O_3-SiO_2-H_2O-TiO_2-O_2 (NCFMKMnASHTO), which models the peak metamorphic conditions for the Mailolo phengite-bearing eclogite. *P–T* pseudosections were calculated with the following solid-solution models (accessible through the Perple_X datafile solution_model.dat): garnet (Gt(WPPH): White et al., 2005); clinopyroxene and amphibole (Omph(GHP2), cAmph(DP2): Diener and Powell, 2012); phengite (Pheng(HP)), biotite (Bio(TCC)), talc (T (HP)), chlorite (Chl(HP)), and epidote (Ep(HP)): Holland and Powell, 1998); ilmenite (Ilm(WPH): White et al., 2000); and feldspar (Fuhrman and Lindsley, 1988). Mineral isopleths calculated by the Perple_X

6.7.0 subprogram Werami are pyrope = Mg/Mg+Ca+Fe+Mn, grossular = Ca/Mg+Ca+Fe+Mn, almandine = Fe/Mg+Ca+Fe+Mn, omphacite jadeite content = Na/Na+Ca, and phengite = Si content based on 11 oxygens. Contours were plotted with the program PyWerami (Ondreij Lexa, personal webpage).

P–T estimates and activity model comparisons

A combination of the Fe–Mg exchange thermometer (Ravna, 2000) and the net-transfer reaction equilibria, 6diopside + 3muscovite = 2grossular + pyrope + 3celadonite, were also used to estimate peak *P–T* (Ravna and Terry, 2004). The following recalculations of garnet, omphacite, and phengite are from the supplemental file of Krogh Ravna and Terry (2004). Garnet was recalculated by normalizing to $\Sigma CaMnFe^{tot}MgAlTiCr = 5.000$, where $Ca + Mn + Fe^{2+} + Mg = 3.000$ and $Al + Ti + Cr + Fe^{3+} = 2.000$. Here $Fe^{3+} = 3.000 – (Al + Ti + Cr)$, and $Fe^{2+} = Fe^{tot} – Fe^{3+}$. Recalculation of omphacite was performed by the same method of the program AX described above, ferric iron calculated assuming 4 cations and 6 oxygens. Phengite has been normalized to $\Sigma SiAlTiCrFeMnMg = 12.000$. The maximum pressure conditions for PNG08-010f was determined with the following mineral compositions: 1) omphacite with the highest jadeite content; 2) garnet with a maximum grossular $(a_{grs})^2a_{prp}$; and 3) phengite with the highest Si content (c.f., Ravna and Terry, 2004).

The *P–T* results from thermobarometry and pseudosection modeling overlap within uncertainty (~10% for both techniques, although these may be underestimated, i.e., Baldwin et al., 2007; Palin et al., 2015). Minimum uncertainties related to thermodynamic and bulk compositional data are taken to be ±0.25 kbar and ±40 °C (e.g., Angiboust et al., 2012; Green et al., 2013; Palin et al., 2015). The pseudosection yields slightly lower pressures in comparison to the thermobarometry, and this likely results from the chosen activity models for clinopyroxene and garnet. The Grt-Cpx-Ph barometer of Krogh Ravna and Terry (2004) uses the clinopyroxene model of Holland and Powell (1990) and garnet model of Ganguly et al. (1996) without taking Fe^{3+}/Fe^{total} into account, whereas the pseudosection models were calculated with more recent garnet (White et al., 2005) and clinopyroxene (Diener et al., 2012) models that do take Fe^{3+}/Fe^{total} into account.

Zr-in-rutile thermometry

Rutile compositions were measured by electron-microprobe analysis with a JEOL JXA-8500F at Washington State University GeoAnalytical Lab using an accelerating voltage of 15 kV, a beam current of 200 nA, and a beam size of 5 μm. Spots for rutile analyses were selected using BSE images and EDS compositional maps. To avoid secondary fluorescence effects from zircon (Ti K-alpha x-rays), rutile grains were selected based on proximity to zircon grains (>200 μm away). Eight elements (Nb, Si, Zr, Ti, Al, V, Cr, Fe) were measured with single spot analyses across 30 rutile grains from eclogite PNG08-010f using the JEOL JXA-8500F at WSU (Table DR2). Counts for zirconium were acquired on two spectrometers and aggregated (c.f., Donovan et al., 2011a). A blank correction was applied to Nb, Zr, Fe, and Si contents using synthetic rutile (~1 ppm, Nb, Zr, Fe, and Si) as the "blank" standard (e.g., Donovan et al., 2011a). An interference correction was applied to correct for interference of Ti Kβ on V Kα, Ti Kβ (III) on Al Kα, and V Kβ on Cr Kα (Donovan et al., 1993).

Temperatures were estimated using the Tomkins et al. (2007) calibration for the coesite field, using a pressure estimate of 28 kbar from pseudosection and thermobarometry results of this study. Analytical uncertainties in Zr measurements range from 2.4–4.5% (1σ) resulting in ±18–31 °C (Table DR2).

U-Pb Thermal-ionization mass spectrometry (TIMS) methodology

Separated zircon from the eclogite sample PNG08-010f were pre-treated following a chemical abrasion procedure (CA-TIMS) modified after Mattinson (2005). This involved annealing the grains at 900 ºC for 60 hours and then placing the individual grains in 200 µl Teflon FEP capsules containing 75 µl concentrated HF at 210 ºC for 9–12 hours to dissolve inclusions and/or radiation-damaged portions of the grains. The leached grains were fluxed on a hot plate and in an ultrasonic cleaner in a series of steps involving Millipore H_2O, 6N HCl, and 3N HNO_3. After rinsing, the grains were dissolved in 75 µl concentrated HF along with the ET535 mixed ^{205}Pb-^{233}U-^{235}U tracer (Condon et la., 2015; McLean et al., 2015) at 210 ºC for 48 hours. The dissolved grains were dried to salts and then redissolved at 180 ºC for 12 hours in 75 µl 6N HCl. Prior to column chemistry, the chloride solution was dried to salts and then redissolved in 50 µl 3N HCl. Pb and U were extracted from the solution by a HCl-based, single-column, anion exchange chemical procedure modified after Krogh (1973). The purified Pb and U mixture was loaded onto a degassed Re filament with a colloidal silica emitter solution (Gerstenberger and Haase, 1997) and their isotopic ratios were measured on either the VG Sector 54 or Isotopx X62 multi-collector thermal ionization mass spectrometers at MIT. Pb isotopes were measured by peak-jumping on a single Daly photomultiplier ion counter. U was measured as UO_2^+ with masses 270, 267, and 265 measured simultaneously on three Faraday detectors. Corrections for Pb-isotope mass fractionation was made based on repeat analyses of NIST SRM981 Pb standard resulting in a fractionation factor of 0.25 %/amu ± 0.04 %/amu (Sector 54) and 0.18 %/amu ± 0.04 %/amu (X62) were applied to single-collector Daly Pb analyses. Use of the ^{233}U-^{235}U double spike allows real time correction for U fractionation.

Data reduction including calculation of U-Pb dates and propagation of uncertainties was carried out using Tripoli and E_T Redux software (Bowring et al., 2011; McLean et al., 2011), using the decay constants of Jaffey et al. (1971).

All common Pb was assumed to be from lab blank and the data were corrected using long-term measured lab blank isotopic compositions compiled from analyses made during 2009–2015. The composition used was ^{206}Pb/^{204}Pb = 18.416 ± 0.475 (1-sigma), ^{207}Pb/^{204}Pb = 15.304 ± 0.295, and ^{208}Pb/^{204}Pb = 37.107 ± 0.875. Total procedural blank is less than 0.1 pg for U. The zircon analyses have been corrected for ^{230}Th disequilibrium by assuming a Th/U ratio of 2.8 ± 1, based on average bulk eclogite analyses from www.earthchem.org. Drastic variation of the assumed Th/U ratio of the fluid from which the zircon (re)crystallized only slightly changes the ^{206}Pb/^{238}U date. For example, if the Th/U ratio for PNG08-010f zircon, z6, is 0.8–4.8, the date varies by a total of ≤ ±20,000 yrs. Complete U-Pb data are presented in Table DR3 and illustrated on the standard Concordia plot of Figure 2B.

References

Bowring, J.F., N.M. McLean, and Bowring, S.A., 2011, Engineering cyber infrastructure for U-Pb geochronology: Tripoli and U-Pb_Redux: Geochem. Geophys. Geosyst., v. 12, Q0AA19, http://dx.doi.org/10.1029/2010GC003479.

Carson, C.J., Powell, R., and Clarke, G.L., 1999, Calculated mineral equilibria for eclogites in CaO-Na_2O-FeO-MgO-Al_2O_3-SiO_2-H_2O: application to the Pouébo Terrane, Pam Peninsula, New Caledonia: Journal of Metamorphic Geology, v. 17, p. 9-24. http://dx.doi.org/10.1046/j.1525-1314.1999.00177.x.

Condon, D.J., Schoene, B., McLean, N.M., Bowring, S.A., and Parrish, R.R., 2015, Metrology and traceability of U-Pb isotope dilution geochronology (EARTHTIME Tracer Calibration Part I): Geochimica Et Cosmochimica Acta, v. 164, p. 464-480.

Connolly, J.A.D., 2005, Computation of phase equilibria by linear programming: A tool for geodynamic modeling and its application to subduction zone decarbonation: Earth and Planetary Science Letters, v. 236, p. 524–541.

Davies, H.L., 1973, Fergusson Island, Papua New Guinea: Geological Series: Australia Bureau of Mineral Resources, Explanatory Notes SC 56/5, scale 1:250,000.

Deer, W.A., Howie, R.A., and Zussman, J., 1992, *An introduction to the rock-forming minerals*, v. 696, London: Longman.

Diener, J.F.A., and Powell, R., 2012, Revised activity-composition models for clinopyroxene and amphibole, Journal of Metamorphic Geology: v. 30, p. 131–142.

Donovan, J.J., Lowers, H.A., and Rusk, B.G., 2011a, Improved electron probe microanalysis of trace elements in quartz: American Mineralogist, v. 96(2-3), p. 274-282.

Donovan, J.J., Snyder, D.A., and Rivers, M.L., 2011b, An improved interference correction for trace element analysis: Microbeam Analysis, v. 2, p. 23-28.

Fuhrman, M.L., and Lindsley, D.H., 1988, Ternary-feldspar modeling and thermometry. American Mineralogist: v. 73(3-4), p. 201-215.

Ganguly, J., Cheng, W., and Tirone, M., 1996, Thermodynamics of aluminosilicate garnet solid solution: new experimental data, an optimized model, and thermometry applications: Contributions to Mineralogy and Petrology, v. 126, p. 137–151.

Gerstenberger, H., and Haase, G., 1997, A highly effective emitter substance for mass spectrometric Pb isotope ratio determinations, Chemical Geology, v. 136, p. 309–312, http://-dx.doi.org/10.1016/S0009-2541(96)00033-2.

Holland, T.J.B., 2009, AX: A Program to Calculate Activities of Mineral End-members from Chemical Analyses. Available at: http://www.esc.cam.ac.uk/research/research-groups/holland/ax (last accessed on 27 October 2015).

Holland, T.J.B. and Powell, R., 1990, An enlarged and updated internally consistent thermodynamic dataset with uncertainties and correlations: The system K2O–Na2O–CaO–

MgO–MnO–FeO–Fe2O3–Al2O3–TiO2–SiO2–C–H2–O2: Journal of Metamorphic Geology, v. 8, p. 89–124.

Holland, T.J.B. and Blundy, J., 1994, Non-ideal interactions in calcic amphiboles and their bearing on amphibole-plagioclase thermometry: Contributions to Mineralogy and Petrology, v. 116, p. 433–447. doi:10.1007/BF00310910.

Holland, T.J.B., and Powell, R., 1998. An internally-consistent thermodynamic dataset for phases of petrological interest: Journal of Metamorphic Geology, v. 16, p. 309-344. http://dx.doi.org/10.1111/j.1525-1314.1998.00140.x.

Indares, A., White, R.W., and Powell, R., 2008. Phase equilibria modelling of kyanite-bearing anatectic paragneisses from the central Grenville Province: Journal of Metamorphic Geology v. 26, p. 815–836. http://dx.doi.org/10.1111/j.1525-

Jackson, S.E., Pearson, N.J., Griffin, W.L., and Belousova, E.A., 2004, The application of laser ablation-inductively coupled plasma-mass spectrometry to in situ U/Pb zircon geochronology: Chemical Geology, v. 211(1–2), p. 47–69, http://dx.doi.org/10.1016/j.chemgeo.-2004.06.017.

Jaffey, A.H., et al., 1971, Precision measurements of half-lives and specific activities of ^{235}U and ^{238}U: Phys. Rev. C., v. 4, p. 1889–1906.

Krogh, T.E., 1973, A low contamination method for hydrothermal decomposition of zircon and extraction of U and Pb for isotopic age determination: Geochim. Cosmochim. Acta., v. 37, p. 485–494.

Locock, A.J., 2014, An Excel spreadsheet to classify chemical analyses of amphiboles following the IMA 2012 recommendations: Computers & Geosciences, v. 62, p. 1–11.

Lexa, Ondrej, 2011, PyWerami: Program to contour and plot in 3D from a contour data file generated by the Perple_X program WERAMI. Available at: http://petrol.natur.cuni.cz/~ondro/pywerami:home (last accessed on 4 November 2016).

Mattinson, J.M., 2005, Zircon U-Pb chemical abrasion ("CA-TIMS") method: combined annealing and multi-step partial dissolution analysis for improved precision and accuracy of zircon ages: Chem. Geol.,v. 220, p. 47–66, http://dx.doi.org/10.1016/-j.chemgeo.2005.03.011.

McLean, N.M., J.F. Bowring, S.A. Bowring, 2011, An algorithm for U-Pb isotope dilution data reduction and uncertainty propagation: Geochem. Geophys. Geosyst., v. 12, Q0AA18, http://dx.doi.org/10.1029/2010GC003478.

McLean, N. M., Condon, D. J., Schoene, B., and Bowring, S. A., 2015, Evaluating uncertainties in the calibration of isotopic reference materials and multi-element isotopic tracers

(EARTHTIME Tracer Calibration Part II): Geochimica Et Cosmochimica Acta, v. 164, p. 481-501.

Palin, R.M., Weller, O.M., Waters, D.J., and Dyck, B., 2016, Quantifying geological uncertainty in metamorphic phase equilibria modelling; a Monte Carlo assessment and implications for tectonic interpretations: Geoscience Frontiers, v. 7(4), p. 591-607.

Proyer, A., Dachs, E. and McCammon, C., 2004, Pitfalls in geothermobarometry of eclogites: Fe3+ and changes in the mineral chemistry of omphacite at ultrahigh pressures: Contributions to Mineralogy and Petrology, v.147, p. 305–318.

Ravna, E. J. K., 2000, The garnet–clinopyroxene geothermometer–an updated calibration: Journal of Metamorphic Geology, v. 18, p. 211–219.

Ravna, E.K., and Terry, M.P., 2004, Geothermometry of UHP and HP eclogites and schists and evaluation of equilibria among garnet-clinopyroxene-kyanite-phengite-coesite/quartz: Journal of Metamorphic Geology, v. 22, p. 579–592, doi:10.1111/j.1525–1314.2004.00534.x.

Wallace, L.M., Stevens, C., Silver, E., McCaffrey, R., Loratung, W., Hasiata, S., Stanaway, R., Curley, R., Rosa, R., and Taugaloidi, J., 2004, GPS and seismological constraints on active tectonics and arc-continent collision in Papua New Guinea: Implications for mechanics of microplate rotations in a plate boundary zone: Journal of Geophysical Research. Solid Earth, v. 109, p. B05404.

White, R. W., Pomroy, N. E., and Powell, R., 2005, An in situ metatexite–diatexite transition in upper amphibolite facies rocks from Broken Hill, Australia: Journal of Metamorphic Geology, v. 23(7), p. 579-602.

Whitney, D.L. and Evans, B.W., 2010, Abbreviations for names of rock-forming mineral: American Mineralogist, v.95, p. 185–187. doi:10.2138/am.2010.3371

SUPPLEMENTARY FIGURE CAPTION

Figure DR1. *P–T* pseudosection from Fig. 3 contoured for mineral isopleths and volume percent of relevant phases showing prograde–retrograde reactions across the entire *P–T* range.

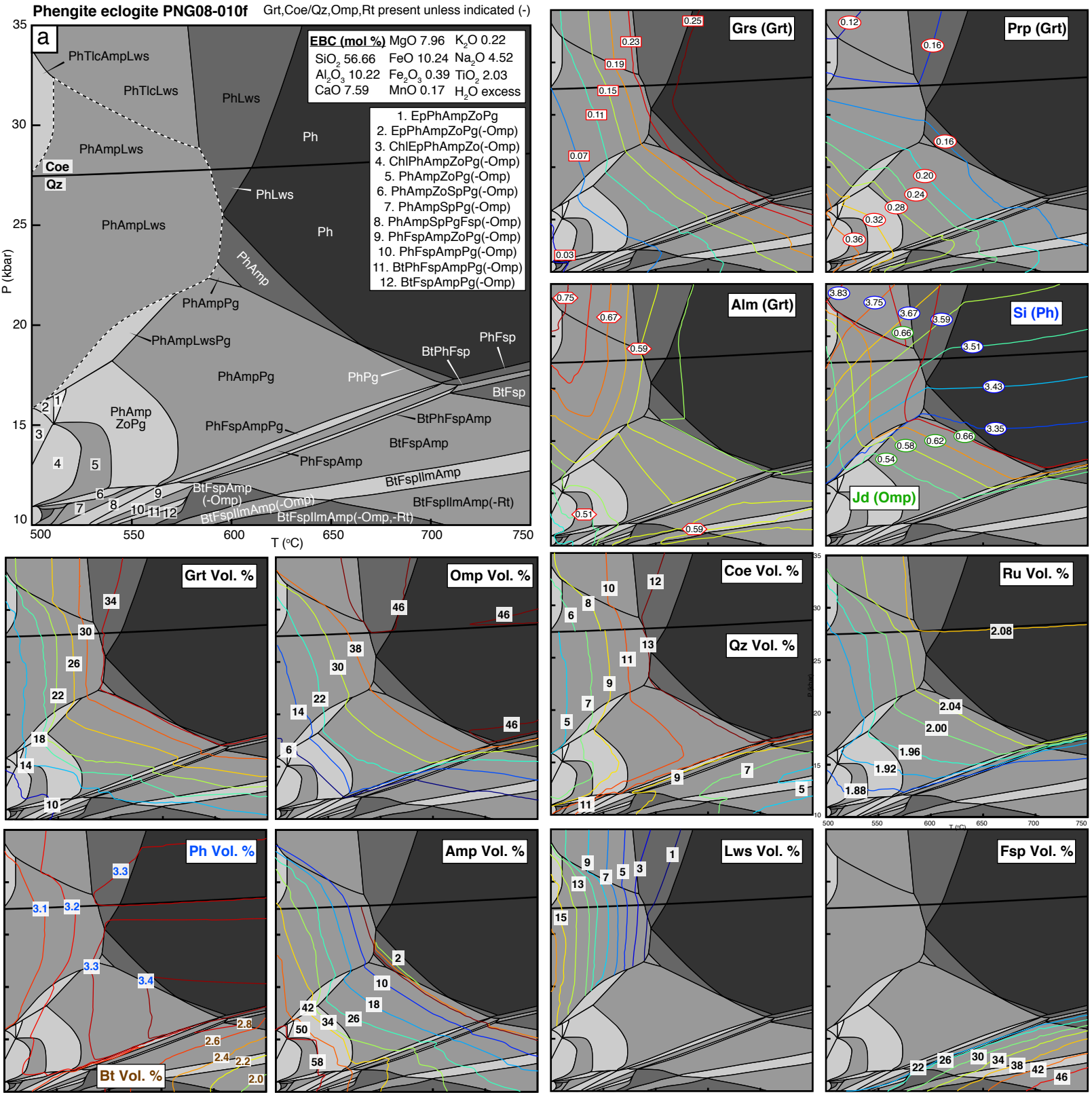

DesOrmeau et al. Figure DR1, DOI:10.1130/G39099.1

Figure DR1. P–T pseudosection from Fig. 3 contoured for mineral isopleths and volume percent of relevant phases showing prograde–retrograde reactions across the entire P–T range.